JOURNAL OF
EMERGING INVESTIGATORS

Article

Enhanced iron and manganese removal using nanocomposite CA/PVP membranes doped with CNC, CNF, and HNT

Deniz Coban[1], Guler Turkoglu-Demirkol[2], Sevgi Gunes-Durak[3]
[1] The Koc School, Istanbul, Turkey
[2] Department of Environmental Engineering, Istanbul University-Cerrahpasa, Istanbul, Turkey
[3] Department of Environmental Engineering, Nevsehir Haci Bektas Veli University, Nevsehir, Turkey

SUMMARY

Iron (Fe) and manganese (Mn) are commonly found in groundwater and surface water sources. When present at elevated concentrations, they can negatively affect drinking water quality by causing aesthetic problems and potential health concerns, including neurological and neurodevelopmental effects. Therefore, the development of efficient and sustainable technologies for the removal of these metals is important. In our study, nanocomposite polymeric membranes were developed to improve the removal of Fe and Mn from drinking water. We incorporated cellulose nanocrystals (CNC), cellulose nanofibers (CNF), and halloysite nanotubes (HNT) into cellulose acetate/polyvinylpyrrolidone (CA/PVP) membranes using the phase inversion method. We evaluated the prepared membranes in terms of water retention capacity, waterflux behavior, and Fe/Mn removal performance. We then conducted filtration experiments using both pure water and surface water collected from Terkos Lake to investigate membrane performance under different water matrices. We hypothesized that CNC-, CNF-, and HNT-doped CA/PVP membranes would exhibit higher permeability and metal removal efficiency than the undoped control membrane. We found that the nanocomposite membranes outperformed the undoped membrane, with CNC-containing membranes showing the best overall filtration performance, and HNT-containing membranes providing enhanced stability during surface water treatment. Overall, our findings indicate that incorporating cellulose-derived nanomaterials and halloysite nanotubes enhanced both the permeability and metal removal performance of CA/PVP membranes. These nanocomposite membranes show strong potential for sustainable drinking water treatment applications targeting Fe and Mn removal.

INTRODUCTION

Iron (Fe) and manganese (Mn) ions are naturally present in ground and surface waters and, despite being essential trace elements, can pose serious health risks when present in excessive concentrations in drinking water. Elevated Mn concentrations have been associated with neurological and neurodevelopmental effects in infants and children, including impaired cognitive function, motor skills, and behavior (1, 2). Mn exposure through drinking water has also been associated with increased infant mortality and long-term neurological toxicity (3, 4). Exposure limit-based risk assessments further indicate that certain subpopulations face non-carcinogenic risk levels well above accepted safety limits when Fe and Mn groundwater concentrations are elevated (5, 6). In addition to these health concerns, Fe imparts a metallic taste and rust color to water, while Mn causes dark coloration and sediment formation in piping systems (7). According to the World Health Organization's (WHO) drinking water quality guidelines, the allowable concentrations of Fe and Mn are 0.3 mg/L and 0.08 mg/L, respectively (8). Concentrations above these limits degrade water quality and increase distribution-system risks, including pipe clogging from Fe/Mn oxide precipitation, biofilm formation by Fe- and Mn-oxidizing bacteria (e.g., Gallionella, Leptothrix), and pathogen growth within these biofilms (9–11). Therefore, developing efficient and sustainable water treatment technologies for Fe and Mn removal is critical to protect public health and ensure safe and palatable drinking water.

Conventional methods such as oxidation, precipitation, and sand filtration have limited success in removing Fe and Mn, particularly at low concentrations or in colloidal form (12). Membrane technologies have therefore come to the forefront due to their high efficiency, modularity, and sustainability. Ultrafiltration (UF) and gravity-driven membrane (GDM) systems in particular offer efficient Fe/Mn removal with low energy requirements (13, 14). However, large-scale applications of membrane technologies still face some limitations, including membrane fouling, low long-term flux, and chemical resistance limitations (15-18). Membrane fouling — the accumulation of organic, inorganic, or microbial matter on the surface and pores — reduces permeability and requires frequent chemical cleaning. Low long-term flux means reduced water throughput per unit area over time, raising the energy and membrane area needed for a given output. Chemical resistance limitations occur when membrane materials degrade under aggressive cleaning agents or oxidants, restricting cleaning protocols and shortening operational lifespan.

Among the various polymers used for membrane fabrication, cellulose acetate (CA) has attracted particular attention due to its high natural abundance, good film-forming ability, high hydrophilicity, biocompatibility, and biodegradability (19). CA-based membranes are widely employed in reverse osmosis, ultrafiltration, and nanofiltration processes owing to their cost-effectiveness, high water flux, chlorine resistance, and favorable antifouling properties (20). They also blend easily with other polymers or nanoparticles to achieve tailored physicochemical properties. Furthermore, as a green, energy-saving biopolymer derived from a renewable resource, CA offers a sustainable alternative to petroleum-based membrane materials, aligning with circular economy principles in water

https://doi.org/10.59720/25-285

treatment (21). Although polymer-based membranes have shown success in metal removal, the number of systems capable of simultaneously removing both Fe and Mn with high efficiency, and in a sustainable manner, remains limited.

Nanomaterial-doped membranes, in which nanomaterials are embedded within the polymer matrix during fabrication to modify its structural and functional properties, offer considerable advantages over conventional polymer matrices by providing higher permeability, fouling resistance, and selectivity. Nanomaterial additives increase the adsorption capacity of metal ions through both physical and chemical modification of the membrane surface (22). These reinforcing nanomaterials include halloysite nanotubes (HNT), tubular aluminosilicate clay minerals with surface functionalization potential; cellulose nanofibers (CNF), flexible nanofibers from lignocellulosic biomass that enhance mechanical strength and hydrophilicity via hydrogen bonding; and cellulose nanocrystals (CNC), rigid rod-like nanoparticles from acid hydrolysis with high elastic modulus and surface-modifiable structure (23, 24). Together, these nanomaterials have enabled the development of nanocomposite membranes with higher surface area, antibacterial properties, chemical resistance, and improved fouling resistance (13, 25–27).

Investigating nanocomposite membranes containing CNC, CNF, and HNT additives may provide valuable insights into optimizing membrane design for efficient Fe and Mn removal in practical drinking water treatment applications. However, the behavior of nano-additives such as HNT, CNF, and CNC during the phase transformation process—their effect on pore morphology, and their capacity to retain metal-ion pairs—has not been studied in detail (28, 29). Previous research has focused primarily on improving permeability or organic pollutant removal rather than specifically targeting Fe/Mn removal from realistic environmental water matrices, and comparative studies evaluating CNC, CNF, and HNT together within the same membrane system, under real surface water conditions, remain particularly scarce.

In this study, we evaluated the performance of nanocomposite membranes developed by integrating HNT, CNF, and CNC into CA/ polyvinylpyrrolidone (PVP)-based polymer matrices for the removal of Fe and Mn ions from water. We hypothesized that nanomaterial-doped membranes, in general, would perform better than the undoped control membrane, with CNC-doped membranes expected to enhance permeability and metal removal. We further hypothesized that combining multiple nanomaterials (CNC, CNF, and HNT) within a single membrane would produce synergistic improvements in filtration performance. To test this, we fabricated the membranes via phase inversion, characterized them for water retention, and performed filtration experiments using both pure water and surface water from Terkos Lake. Our results revealed that CNC-doped membranes achieved over 90% removal for both metals, while HNT-doped membranes provided the highest flux stability under surface water conditions. Our findings demonstrate that selecting nanomaterials based on water structure can substantially optimize membrane performance for sustainable drinking water treatment, contributing to current research on environmental sustainability and the technological potential of nanomaterial-modified membranes for metal ion removal.

RESULTS

Our work evaluated the performance of nanocomposite CA/PVP membranes doped with CNC, CNF, and HNT for the removal of Fe and Mn from water. For comparison, we also fabricated CA/dimethylformamide (DMF) membranes, in which DMF was used as an alternative to N-methyl-2-pyrrolidone (NMP), the solvent used to fabricate the other membranes,

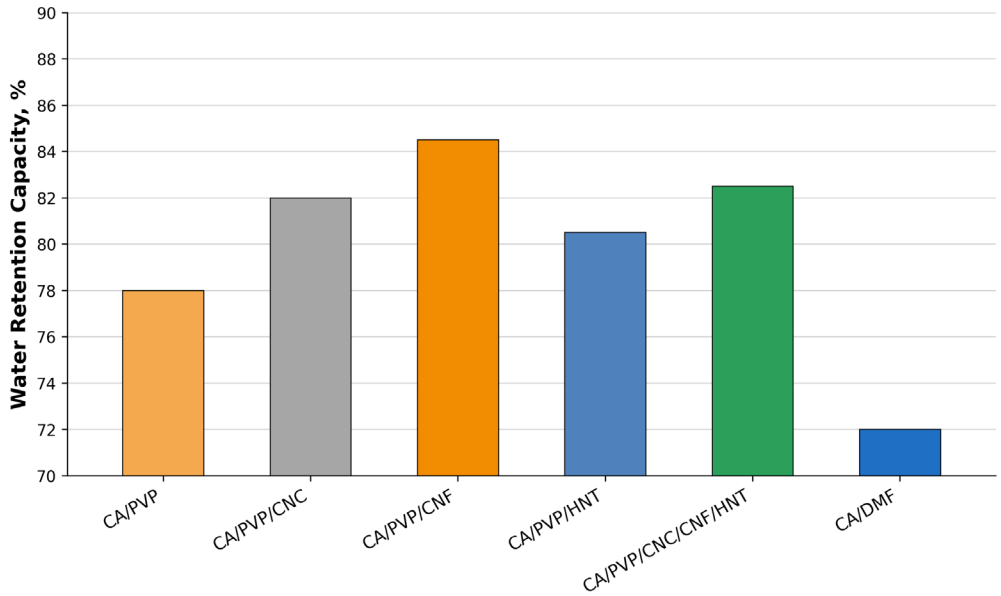

Figure 1. Water retention capacity results. Water retention capacity (%) of cellulose acetate/dimethylformamide (CA/DMF), cellulose acetate/polyvinylpyrrolidone (CA/PVP), cellulose nanocrystal (CNC)-doped, cellulose nanofiber (CNF)-doped, halloysite nanotube (HNT)-doped, and multi-doped CA/PVP/CNC/CNF/HNT membranes. CNC- and CNF-containing membranes exhibited the highest water retention capacities (~82–85%).

https://doi.org/10.59720/25-285

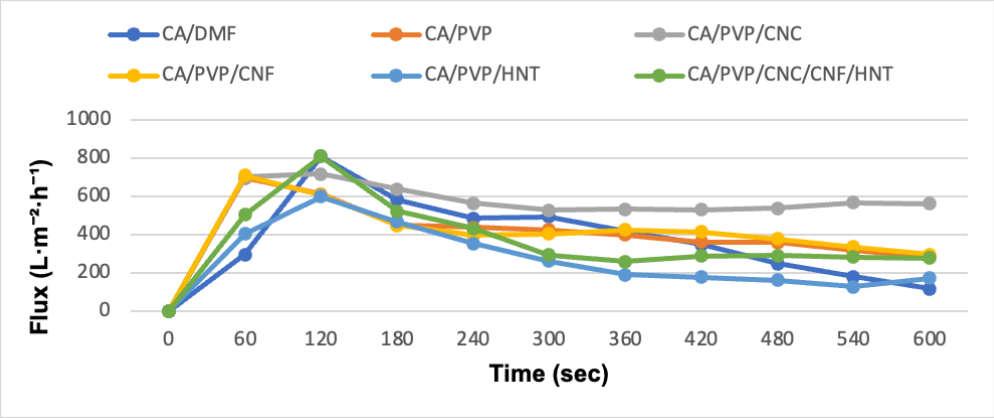

Figure 2. Flux stability of neat and nanomaterial-doped membranes under pure water conditions. Flux (L m^{-2} h^{-1}) was measured over time during dead-end filtration of pure water at 1.2 bar using cellulose acetate/dimethylformamide (CA/DMF), cellulose acetate/polyvinylpyrrolidone (CA/PVP), cellulose nanocrystal (CNC)-doped, cellulose nanofiber (CNF)-doped, halloysite nanotube (HNT)-doped, and multi-doped CA/PVP/CNC/CNF/HNT membranes.

and no PVP pore-forming agent was included; while this control does not isolate the individual effects of solvent choice and PVP incorporation, it served as a general baseline against which the nanomaterial-doped membranes could be compared. We characterized the fabricated membranes through water retention and permeability measurements, followed by filtration experiments using both pure water and surface water from Terkos Lake.

Water Retention Capacity

We measured water retention capacity to assess membrane hydrophilicity and pore structure, both of which influence flux and metal removal performance. All membranes showed high water retention capacity in pure water, generally above 70% **(Figure 1)**. CNF- and CNC-doped membranes showed the highest retention (~85% each), followed by the multi-additive membrane (~82%) and HNT-doped membranes (~81%), both above the undoped control (~78%). The lowest retention was observed for the CA/DMF membrane (~72%).

Pure Water and Lake Water Flux

We used flux measurements under both pure water and surface water conditions to evaluate membrane permeability and fouling resistance over time. The results obtained from pure water filtration experiments show that initial fluxes were high across all membranes, but considerable performance differences emerged over time (**Figure 2**). Under pure water conditions, the CA/PVP/CNC membrane performed the best among all tested membranes **(Figure 2)**. While its initial flux (~700 L·m^{-2}·h^{-1}) was comparable to that of the neat CA/PVP membrane (~700 L·m^{-2}·h^{-1}), the CA/PVP/CNC membrane retained a substantially higher flux of 560 L·m^{-2}·h^{-1} after 600 seconds, compared to only 180 L·m^{-2}·h^{-1} for the neat CA/PVP membrane. The CA/PVP/CNF (730→370 L·m^{-2}·h^{-1}) and CA/DMF (810→118 L·m^{-2}·h^{-1}) membranes showed intermediate to low stability, while the CA/PVP/HNT membrane exhibited the lowest pure-water performance (620→100 L·m^{-2}·h^{-1}). The CA/PVP/CNC/CNF/HNT multi-additive membrane reached the highest initial flux among all membranes (~810 L·m^{-2}·h^{-1}) but

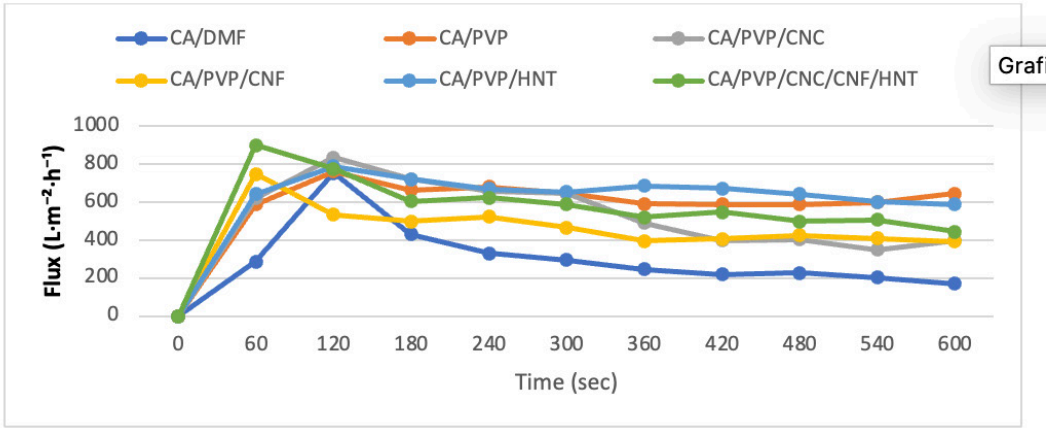

Figure 3. Flux stability of neat and nanomaterial-doped membranes under Terkos Lake water conditions. Flux (L m^{-2} h^{-1}) was measured over time during dead-end filtration of Terkos Lake water at 1.2 bar using cellulose acetate/dimethylformamide (CA/DMF), cellulose acetate/polyvinylpyrrolidone (CA/PVP), cellulose nanocrystal (CNC)-doped, cellulose nanofiber (CNF)-doped, halloysite nanotube (HNT)-doped, and multi-doped CA/PVP/CNC/CNF/HNT membranes.

https://doi.org/10.59720/25-285

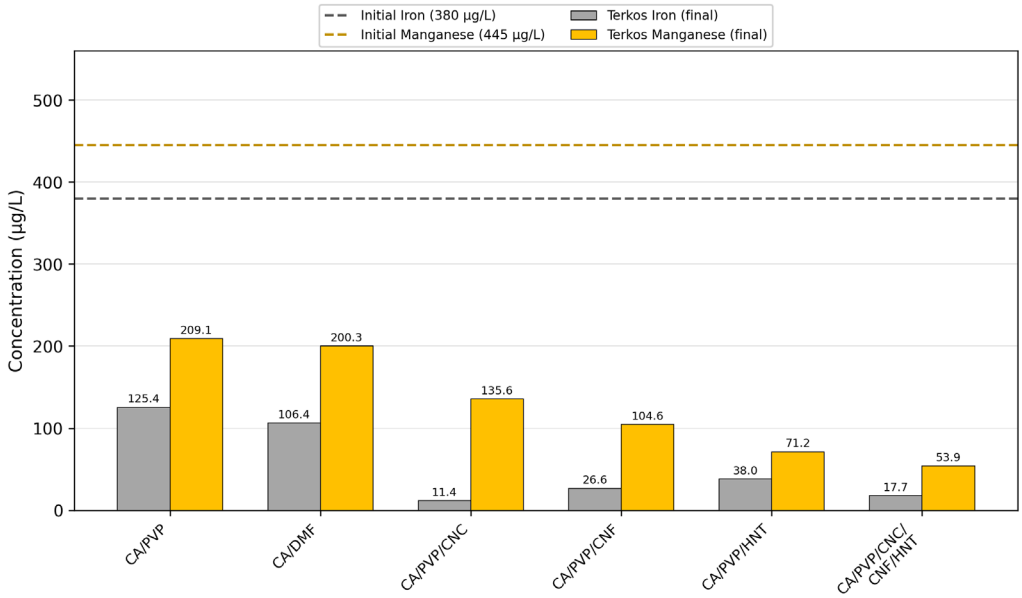

Figure 4. Iron (Fe) and manganese (Mn) concentrations before and after treatment with the fabricated membranes. Comparison of Fe and Mn concentrations measured in Terkos Lake water before filtration and after treatment using cellulose acetate/dimethylformamide (CA/DMF), cellulose acetate/polyvinylpyrrolidone (CA/PVP), cellulose nanocrystal (CNC)-doped, cellulose nanofiber (CNF)-doped, halloysite nanotube (HNT)-doped, and multi-doped CA/PVP/CNC/CNF/HNT membranes. Initial Fe and Mn concentrations were 380 µg/L and 445 µg/L, respectively.

declined to 278 $L \cdot m^{-2} \cdot h^{-1}$ by 600 seconds. This indicates that CNC doping positively affects flux stability compared to the undoped control and other nanomaterial-doped membranes.

Under surface water conditions (Terkos Lake), the CA/PVP/HNT membrane — rather than the CNC-doped membrane — was the most stable performer **(Figure 3)**. The CA/PVP/CNC membrane reached a peak flux of ~820 $L \cdot m^{-2} \cdot h^{-1}$ at 120 s but declined steadily thereafter to ~400 $L \cdot m^{-2} \cdot h^{-1}$ by 600 s, while the CA/PVP/CNF membrane peaked earlier (~780 $L \cdot m^{-2} \cdot h^{-1}$ at 60 s) and declined to ~410 $L \cdot m^{-2} \cdot h^{-1}$ by 600 s. The CA/DMF membrane performed worst, declining from ~750 to only 170 $L \cdot m^{-2} \cdot h^{-1}$. The CA/PVP/CNC/CNF/HNT membrane reached the highest initial flux (~900 $L \cdot m^{-2} \cdot h^{-1}$) but declined to 450 $L \cdot m^{-2} \cdot h^{-1}$ by 600 seconds. The CA/PVP membrane showed an initial flux of ~600 $L \cdot m^{-2} \cdot h^{-1}$, rising to a peak of ~780 $L \cdot m^{-2} \cdot h^{-1}$ at 120 s before stabilizing around 650 $L \cdot m^{-2} \cdot h^{-1}$ through 600 s. The CA/PVP/HNT membrane was the most stable, with an initial flux of ~641 $L \cdot m^{-2} \cdot h^{-1}$ that remained relatively stable through 600 seconds. This suggests that HNT doping strengthens membrane stability.

Iron and Manganese Removal

We measured Fe and Mn concentrations using atomic absorption spectroscopy (AAS) before and after filtration to directly evaluate each membrane's effectiveness for the target application: removal of these metals from drinking water. The initial concentrations of Fe and Mn in Terkos Lake water prior to filtration experiments were 380 µg/L and 445 µg/L, respectively.

These concentrations decreased substantially after membrane treatment, though the extent varied by membrane type **(Figure 4)**. The CA/PVP membrane reduced Fe and Mn concentrations to 125 and 209 µg/L (67% and 53% removal), while the CA/DMF membrane achieved comparable efficiencies (Fe: 106 µg/L, 72%; Mn: 200 µg/L, 55%) **(Figure 4)**. Among the nanomaterial-doped membranes, the CA/PVP/CNC membrane provided the highest removal efficiency (Fe: 11 µg/L, 97%; Mn: 136 µg/L, 70%). The CA/PVP/CNF membrane reduced Fe to 26.6 µg/L and Mn to 104.6 µg/L (93% and 76.5% removal). The CA/PVP/HNT membrane reduced Fe to 38 µg/L and Mn to 71.2 µg/L (90% and 84% removal). The multi-doped CA/PVP/CNC/CNF/HNT membrane reduced Fe to 17.7 µg/L and Mn to 53.9 µg/L (>95% and 88% removal) (**Figure 4**).

DISCUSSION

In this work, we evaluated the performance of nanocomposite CA/PVP membranes doped with different nanomaterials (CNC, CNF, and HNT) for the removal of Fe and Mn from water. We hypothesized that CNC-doped membranes would exhibit higher metal removal efficiency due to their enhanced hydrophilicity and adsorption capacity, and that nanomaterial-doped membranes in general would perform better than the undoped control membrane. To explore this hypothesis, we evaluated the water retention, permeability, and filtration capacity of fabricated membranes using pure water and surface water from Terkos Lake. We included a CA/DMF membrane, prepared without PVP or nanomaterial doping, as a baseline against which the nanomaterial-doped membranes could be compared.

Water retention and flux, though measuring different aspects of membrane behavior, are mechanistically linked: higher retention generally reflects greater hydrophilicity, which reduces resistance to water transport and supports higher

https://doi.org/10.59720/25-285

flux, whereas low-retention (more hydrophobic) membranes tend to foul more readily, compromising flux stability over time. Both parameters are therefore evaluated together, since permeability gains from high retention can be offset by reduced fouling resistance, or vice versa, depending on the additive and application context (34, 35).

The results suggest that nanomaterial incorporation may influence several structural and functional properties of CA-based membranes. In particular, cellulose-derived nanomaterials (CNC and CNF) appeared to increase water retention capacity, likely due to the abundant hydroxyl groups in their chemical structure (36). These functional groups may enhance interactions with water molecules, improving membrane hydrophilicity. In our study, CNC- and CNF-doped membranes reached water retention values of ~85%, and the multi-doped CA/PVP/CNC/CNF/HNT membrane reached ~82%, consistent with previously reported nanomaterial-modified membranes (37). Similar findings in the literature support that the hydrophilic character of cellulose-derived nanomaterials noticeably increases the water retention capacity and water filtration performance (28, 38). These findings support our hypothesis that cellulose-derived nanomaterials (CNC, CNF) would increase hydrophilicity and water retention compared to the undoped control membrane.

While previous studies have primarily emphasized CNC and CNF's role in improving pore structure and organic contaminant removal, our findings suggest these nanomaterials may also aid heavy metal ion (Fe, Mn) adsorption: the same hydroxyl groups responsible for increased hydrophilicity and water retention can act as complexation/ion-exchange sites for metal cations, while greater water uptake may enhance ion accessibility to these sites (37, 39). The slightly lower retention of the multi-doped membrane (~82%) compared to single-additive CNC or CNF membranes suggests that combining multiple nanomaterials may cause partial competition for pore volume rather than a fully synergistic effect, potentially reducing structural homogeneity (40). This implies that nanomaterial selection needs to be optimized rather than maximized in number. Similarly, the comparatively higher retention of HNT-doped membranes (~81%) relative to the control—despite HNT's lower intrinsic hydrophilicity—suggests that its tubular morphology may contribute more to mechanical reinforcement and antifouling behavior than to water affinity, a distinction that may guide future additive selection depending on whether flux stability or metal-ion adsorption capacity is the primary design goal (32, 33).

Additionally, the low water retention capacity observed for the CA/DMF membrane (~72%) in the absence of PVP is consistent with earlier reports on solvent effects in CA-based membrane fabrication. During phase inversion — where a cast polymer solution solidifies into a porous membrane upon immersion in a non-solvent bath — solvent choice strongly influences the resulting pore structure. Porosity and water flux in NMP-based CA membranes increase considerably with higher PVP (pore-forming additive) content, because NMP's high compatibility with CA promotes a uniform, well-connected pore network (41). DMF, the solvent used in our PVP-free control membrane, behaves differently: in a related polymer, DMF has been shown to promote a more compact, crystalline chain arrangement and to alter the membrane's thermal and mechanical behavior (42). A more compact, crystalline structure that leaves less room for interconnected pores, along with the absence of PVP, may help explain the comparatively lower porosity and hydrophilicity we observed for the CA/DMF membrane relative to the CA/PVP membranes in this study.

Water flux experiments further suggest that the influence of nanomaterials may depend strongly on the filtration environment. Under pure water conditions, the CA/PVP/CNC membrane exhibited relatively high and stable flux values, which may be associated with increased membrane porosity and hydrophilicity resulting from CNC incorporation. However, when filtration experiments were conducted using Terkos Lake water, the flux declined more sharply than under pure water conditions, possibly due to the presence of natural organic matter, suspended particles, and dissolved ions that can contribute to membrane fouling. Under these conditions, the CA/PVP/HNT membrane maintained comparatively stable flux values. This observation may suggest that the tubular morphology and surface characteristics of HNT contribute to improved structural stability and fouling resistance under more complex water matrices (32, 33). In contrast, the CA/DMF membrane exhibited the sharpest flux decline under both pure and lake water conditions, consistent with the reduced pore density and connectivity associated with DMF-based phase separation and the reduced hydrophilicity resulting from the absence of PVP doping (43). Together, these results indicate that additive selection should be guided by the intended water source — CNC for high-purity feedwaters, HNT for fouling-prone surface waters.

The heavy metal removal experiments also provide insights into the role of nanomaterial additives. The comparatively limited performance of the CA/PVP and CA/DMF membranes (67–72% Fe, 53–55% Mn removal) was likely due to poorer pore structure and lower hydrophilicity from the absence or insufficiency of additives, underscoring that nanomaterial doping — not the base polymer alone — governs metal-ion removal capacity (44). The CA/PVP/CNC membrane achieved the highest Fe removal (97%), likely due to CNC's increased surface area, improved hydrophilicity, and enhanced metal-ion interaction — partially supporting our hypothesis that CNC doping would enhance metal removal. However, this effect was more pronounced for iron than manganese, as CNC's Mn removal (70%) was comparatively lower than that of the CNF-, HNT-, and multi-doped membranes (45, 46). The CA/PVP/CNF membrane's performance may relate to the hydroxyl (–OH) groups on its cellulose chains (47–49). By contrast, the CA/PVP/HNT membrane achieved higher manganese removal (84%) than CNC or CNF alone, which may be associated with the surface hydroxyl (Al–OH) and silanol (Si–OH) groups characteristic of HNT as well as its tubular structure and charge-balancing capacity (40, 44). The multi-doped CA/PVP/CNC/CNF/HNT membrane achieved the highest combined removal profile (>95% Fe, 88% Mn), suggesting that combining nanomaterials may optimize membrane porosity, surface area, and ion-binding properties simultaneously — an outcome with practical relevance for designing membranes that must remove multiple contaminants at once, as is typical of real-world surface water treatment (37, 50). These values compare favorably with previous membrane-based approaches for Fe/Mn removal. Pre-chlorination combined with UF treatment

https://doi.org/10.59720/25-285

achieved up to 80% Mn removal, though membrane clogging increased with chlorine dose (13). Long-term gravity-driven membrane (GDM) filtration achieved 94.6% Mn removal with low flux (6.3 $L \cdot m^{-2} \cdot h^{-1}$) (51) especially in the complex cases of organics involvement. Gravity-driven membrane (GDM. Biofilm-assisted GDM systems achieved nearly 90% Fe and 58% Mn removal (52). Compared to these values, the HNT-doped membrane in our study achieved a similar level of Fe removal (90%) without requiring pre-chlorination or biofilm accumulation, while reaching a considerably higher Mn removal efficiency (84% vs. 58%), suggesting that nanomaterial doping may offer a more practical and efficient alternative to conventional GDM-based approaches.

One limitation of this study is that filtration experiments were conducted under fixed pH and temperature conditions specific to a single real water source (Terkos Lake) collected at one point in time, and flux stability was assessed only over 600 seconds. This is relevant because Fe and Mn adsorption/oxidation behavior is strongly pH-dependent, with higher pH generally promoting insoluble metal oxide formation and increasing adsorption capacity (53). Temperature can similarly affect reaction kinetics, diffusion rates, and membrane transport properties (54). Since natural water sources vary considerably in pH, temperature, and composition across seasons and locations, the removal efficiencies reported here may not generalize to sources with substantially different characteristics or to longer-term operation. Future studies systematically varying pH, temperature, and testing duration across multiple water matrices would help clarify the generalizability of our findings.

Two further limitations concern our mechanistic interpretations and the reproducibility of our results. Our interpretations regarding the roles of CNC, CNF, and HNT in enhancing porosity, hydrophilicity, and metal-ion interactions were inferred from performance data (flux, retention, removal efficiency) rather than direct structural characterization; techniques such as SEM, surface porosity analysis, and contact angle measurements would be needed to substantiate these interpretations, and their absence limits the causal claims that can be drawn. In addition, we did not replicate measurements across multiple independent membrane batches, so reproducibility has not yet been statistically established. Addressing these limitations — through advanced characterization, replicated experiments, long-term/pilot-scale trials under realistic conditions, and computational modeling of nanomaterial–metal ion interactions — would strengthen confidence in the proposed mechanisms and support next-generation nanocomposite membranes with optimized permeability, adsorption capacity, and fouling resistance.

Overall, our findings suggest that CNC may serve as a versatile additive enhancing permeability and metal removal, whereas HNT may improve flux stability and fouling resistance under more complex water conditions. This highlights that nanomaterial selection should be tailored to the intended application rather than relying on a single additive. From a practical standpoint, CNC-doped membranes may be well-suited for treating relatively clean source waters where high permeability is the priority, such as pre-treated groundwater, whereas HNT-doped membranes may be more appropriate for decentralized or point-of-use systems drawing directly from surface water sources — such as lakes and reservoirs — where fouling resistance is critical for consistent long-term performance. Given that Fe and Mn contamination is a common challenge for communities relying on surface water, particularly where advanced treatment infrastructure is limited, nanocomposite membranes of this type could offer a low-cost, chemical-free alternative to conventional pre-chlorination or biofilm-based approaches. Notably, filtered water concentrations in this study were below WHO guideline values, indicating that these membranes could already meaningfully improve drinking water quality even prior to further optimization. With further optimization and pilot-scale validation, this approach may support more accessible and sustainable drinking water treatment for communities facing Fe and Mn contamination.

MATERIALS AND METHODS

Fabrication of the Membranes

All membranes were fabricated using the phase inversion method. In the membrane fabrication process, CA (Sigma-Aldrich) was used as the polymer, and NMP (Merck) and DMF (Merck) were used as solvents. PVP (Sigma-Aldrich) was used as a pore-forming agent. HNT (Nanography; diameter 30–70 nm, length 1–3 μm), CNF (Nanography; diameter 10–20 nm, length 2–3 μm), and CNC (Nanography; width 10–20 nm, length 300–900 nm) were used as reinforcement nanomaterials (**Table 1**). Although the fabrication procedure involves similar steps for all membrane types, the order and proportions of additives vary.

In fabricating neat membranes, polymer composition was fixed at 16 wt% CA and 5 wt% PVP (**Table 2**). PVP was dissolved in NMP at 60 °C, followed by CA. The mixture was stirred at 60 °C until homogeneous and sonicated at 25 °C for 30 min prior to casting. Membranes were cast as 200 μm films, immersed in a pure water coagulation bath, and stored in pure water at 4 °C for 48 h to remove residual impurities and stabilize structure following phase inversion. A similar procedure was applied for the CA/PVP/DMF system; however, preliminary mechanical strength and filtration performance evaluations showed NMP-based membranes outperformed DMF-based ones. Therefore, NMP was selected for the fabrication of nanocomposite membranes. In addition to the NMP-based nanocomposite membranes, a PVP-free CA/DMF control membrane was fabricated to serve as a baseline against which the nanomaterial-doped membranes could be compared. CA (16 wt%) was dissolved directly in DMF at 60 °C without PVP, stirred until homogeneous, and sonicated at 25 °C for 30 min prior to casting. The solution was cast as a 200 μm film, immersed in a pure water coagulation bath, and stored in pure water at 4 °C for 48 h, consistent with the other membranes.

Fabrication of Nanomaterial-doped Composite Membranes

For the CA/PVP/CNF membrane, 0.75 g CNF was dispersed in 79 g NMP at 60 °C, followed by 5 g PVP and 16 g CA. The mixture was stirred for 24 h, sonicated for 30 min, and cast. The same procedure was followed for the CA/CNC and CA/HNT membranes, substituting 0.75 wt% CNC or HNT for CNF. For the multi-additive CA/PVP/CNC/CNF/HNT

https://doi.org/10.59720/25-285

Materials	Company	Molecular Weight (g/mol)	Intended Use
Cellulose acetate (CA)	Sigma-Aldrich	50,000	Polymer
Polyvinylpyrrolidone (PVP)	Sigma-Aldrich	10,000	Pore-forming polymer
1-Methyl-2-Pyrrolidone (NMP)	Merck	99.13	Solvent
Dimethylformamide (DMF)	Merck	73.09	Solvent
Cellulose nanofiber (CNF)	Nanography	-	Nanomaterial
Halloysite nanotubes (HNT)	Nanography	-	Nanomaterial
Cellulose nanocrystal (CNC)	Nanography	-	Nanomaterial

Table 1. Materials used in membrane fabrication. List of polymers, solvents, pore-forming agents, and nanomaterials utilized in membrane preparation. Molecular weight is not applicable to nanomaterials; see Methods for particle dimensions.

Membrane code	Composition (wt.%)						
	CA	PVP	NMP	DMF	CNC	CNF	HNT
CA/PVP/NMP	16	5	79	-	-	-	-
CA/PVP/DMF	16	5	-	79	-	-	-
CA/PVP/CNC	16	5	78.25	-	0.75		-
CA/PVP/CNF	16	5	78.25	-	-	0.75	-
CA/PVP/HNT	16	5	78.25	-	-	-	0.75
CA/PVP/CNC/CNF/HNT	16	5	78.25	-	0.25	0.25	0.25

Table 2. Composition of membrane casting solutions. Polymer, solvent, and nanomaterial weight percentages used in the preparation of cellulose acetate/dimethylformamide (CA/DMF), cellulose acetate/polyvinylpyrrolidone (CA/PVP), cellulose nanocrystal (CNC)-doped, cellulose nanofiber (CNF)-doped, halloysite nanotube (HNT)-doped, and multi-doped CA/PVP/CNC/CNF/HNT membranes.

membrane, 0.25 g each of CNC, CNF, and HNT were added to NMP and mixed at 60 °C, followed by 5 g PVP and 16 g CA. The solutions were stirred until homogeneous. Before casting, all solutions were sonicated for 30 min and membranized following the standard procedure. All membranes were stabilized in pure water at 4 °C for 48 h and fabricated to an average size of ~6 cm × 20 cm.

Calculation of Water Retention Capacity

Water retention capacity was determined from the difference between wet and dry membrane weights: membranes were dried in an oven (NUVE EN 500, 24 h, 60 °C) and weighed (Kern 573), then immersed in pure water and reweighed after removing excess surface water with blotting paper. Water retention capacity was calculated using **Equation 1**:

$$\text{Water retention capacity (\%)} = \frac{W_{wet} - W_{dry}}{W_{wet}} \times 100$$

Calculation of Water Permeability Performance of Membranes

Membrane permeability was measured using a continuously stirred, nitrogen-driven dead-end filtration system (Tin Engineering; 300 mL cell, 5 cm membrane diameter). Membranes were pre-conditioned with pure water at 1.2 bar for 10 min to stabilize flux and open pores. For flux measurements, water was passed through the membrane at the same pressure and collected in a beaker on a precision balance. The flux (J; $L \cdot m^{-2} \cdot h^{-1}$) *was calculated using* **Equation 2**:

$$J = \frac{V}{A\,\Delta t}$$

https://doi.org/10.59720/25-285

where V is the permeate volume (L), A is the effective membrane surface area (m²), and Δt is the filtration time (h). The same equation was used for fouled conditions, substituting the permeate volume from Terkos Lake water filtration; no correction terms were applied, as we aimed to characterize observed (rather than intrinsic) flux as fouling progressed.

Measurement of Fe and Mn concentrations

Samples were collected before filtration (feed) and from the filtrate (permeate) for each membrane. Fe and Mn concentrations in the feed and permeate streams were determined by comparing absorbance readings measured in a flame AAS (PerkinElmer) to a calibration curve prepared from known Fe and Mn standards. Concentrations were determined in µg/L.

Calculation of Fe and Mn removal efficiencies of membranes

Membrane removal efficiency for Fe and Mn is a dimensionless measure (R, between 0 and 1) of the material retained by the membrane, with R = 1 indicating 100% removal. Observed removal efficiency, calculated from the filtrate and feed stream concentrations, differs from actual removal efficiency, which depends on the concentration at the membrane surface. In this study, observed removal efficiency (R_o) was calculated using **Equation 3.**

$$R_o\ (\%) = \frac{Cf - Cp}{Cf} x100$$

where Cf is the feed concentration and Cp is the permeate concentration.

Received: September 22, 2025
Accepted: April 1, 2026
Published: August 25, 2026

REFERENCES

1. Ljung, Karin, et al. “Time to Re-Evaluate the Guideline Value for Manganese in Drinking Water?” Environmental Health Perspectives, vol. 115, no. 11, Nov. 2007, pp. 1533–38. https://doi.org/10.1289/ehp.10316.
2. Ramachandran, Maithili, et al. “Shallow Groundwater Manganese Merits Deeper Consideration.” Environmental Science & Technology, vol. 55, no. 6, Mar. 2021, pp. 3465–66. https://doi.org/10.1021/acs.est.0c08065.
3. Hafeman, Danella, et al. “Association between Manganese Exposure through Drinking Water and Infant Mortality in Bangladesh.” Environmental Health Perspectives, vol. 115, no. 7, July 2007, pp. 1107–12. https://doi.org/10.1289/ehp.10051.
4. Scher, Deanna P., et al. “Potential for Manganese-Induced Neurologic Harm to Formula-Fed Infants: A Risk Assessment of Total Oral Exposure.” Environmental Health Perspectives, vol. 129, no. 4, Apr. 2021, p. 047011. https://doi.org/10.1289/EHP7901.
5. Ghosh, Gopal Chandra, et al. “Human Health Risk Assessment of Elevated and Variable Iron and Manganese Intake with Arsenic-Safe Groundwater in Jashore, Bangladesh.” Scientific Reports, vol. 10, no. 1, Mar. 2020, p. 5206. https://doi.org/10.1038/s41598-020-62187-5.
6. Chakraborty, Tapos Kumar, et al. “Arsenic, Iron, and Manganese in Groundwater and Its Associated Human Health Risk Assessment in the Rural Area of Jashore, Bangladesh.” Journal of Water and Health, vol. 20, no. 6, June 2022, pp. 888–902. https://doi.org/10.2166/wh.2022.284.
7. Browning, Emily G., et al. “Manganese and Iron in Drinking Water in Three West-African Countries: Implications for Health, Acceptability, and Disinfection.” PLOS Water, vol. 4, no. 6, June 2025, p. e0000234. https://doi.org/10.1371/journal.pwat.0000234.
8. Guidelines for Drinking-Water Quality: Fourth Edition Incorporating the First and Second Addenda. https://www.who.int/publications/i/item/9789240045064. Accessed 29 Oct. 2025.
9. Sharma, Saroj K. Adsorptive Iron Removal from Groundwater. Swets & Zeitlinger, PhD Thesis, Wageningen University/IHE Delft, The Netherlands, 2001.
10. Katsoyiannis, Ioannis, et al. “Biological Treatment of Mn(II) and Fe(II) Containing Groundwater: Kinetic Considerations and Product Characterization.” Water Research, vol. 38, no. 7, Apr. 2004. https://doi.org/10.1016/j.watres.2004.01.014.
11. Li, Guiwei, et al. “Deposit Accumulation and Release under Drinking Water Conditions: Differences between Manganese and Iron and the Impact of Pipe Materials.” ACS ES&T Water, vol. 5, no. 11, Nov. 2025, pp. 6544–53. https://doi.org/10.1021/acsestwater.5c00640.
12. Simate, Geoffrey S., et al. “Acid Mine Drainage: Challenges and Opportunities.” Journal of Environmental Chemical Engineering, vol. 2, no. 3, Sept. 2014, pp. 1785–803. https://doi.org/10.1016/j.jece.2014.07.021.
13. Choo, Kwang-Ho, et al. “Iron and Manganese Removal and Membrane Fouling during UF in Conjunction with Prechlorination for Drinking Water Treatment.” Journal of Membrane Science, vol. 267, no. 1, Dec. 2005, pp. 18–26. https://doi.org/10.1016/j.memsci.2005.05.021.
14. Boersma, Alje S., et al. “Influence of Filter Backwashing on Iron, Manganese, and Ammonium Removal in Dual-Media Rapid Sand Filters Used for Drinking Water Production.” Water Research, vol. 270, Feb. 2025, p. 122809. https://doi.org/10.1016/j.watres.2024.122809.
15. Madaeni, S. S. “The Application of Membrane Technology for Water Disinfection.” Water Research, vol. 33, no. 2, Feb. 1999, pp. 301–08. https://doi.org/10.1016/S0043-1354(98)00212-7.
16. Lin, Dachao, et al. “Enhanced Membrane Fouling by Microplastics during Nanofiltration of Secondary Effluent Considering Secretion, Interaction and Deposition of Extracellular Polymeric Substances.” Science of The Total Environment, vol. 906, Jan. 2024, p. 167110. https://doi.org/10.1016/j.scitotenv.2023.167110.
17. Shen, Maocai, et al. “Recent Advances on Micro/Nanoplastic Pollution and Membrane Fouling during Water Treatment: A Review.” Science of The Total Environment, vol. 881, July 2023, p. 163467. https://doi.org/10.1016/j.scitotenv.2023.163467.

18. Su, Minghan, et al. "Challenges and Solutions for Nanofiltration Membranes in Water Treatment." Frontiers in Chemical Engineering, vol. 7, Oct. 2025. https://doi.org/10.3389/fceng.2025.1695014.
19. An, Yaxin, et al. "Hydrophobic Modification of Cellulose Acetate and Its Application in the Field of Water Treatment: A Review." Molecules, vol. 29, no. 21, Jan. 2024, p. 5127. https://doi.org/10.3390/molecules29215127.
20. Islam, Md. Didarul, et al. "Cellulose Acetate-Based Membrane for Wastewater Treatment—A State-of-the-Art Review." Materials Advances, vol. 4, no. 18, Sept. 2023, pp. 4054–102. https://doi.org/10.1039/d3ma00255a.
21. Oprea, Madalina, et al. "Cellulose Acetate-Based Materials for Water Treatment in the Context of Circular Economy." Water, vol. 15, no. 10, Jan. 2023, p. 1860. https://doi.org/10.3390/w15101860.
22. Agboola, Oluranti, et al. "A Review on Polymer Nanocomposites and Their Effective Applications in Membranes and Adsorbents for Water Treatment and Gas Separation." Membranes, vol. 11, no. 2, Feb. 2021, p. 139. https://doi.org/10.3390/membranes11020139.
23. Rana, Rinku, et al. "Nanocellulose/Nanocellulose-Based Membranes in Wastewater Treatment: A Sustainable Path Forward for Environmental Protection." Food Chemistry: X, vol. 29, July 2025, p. 102654. https://doi.org/10.1016/j.fochx.2025.102654.
24. Abid, Mahmoud, et al. "Halloysite-TiO2 Nanocomposites for Water Treatment: A Review." Nanomaterials, vol. 13, no. 9, Jan. 2023, p. 1578. https://doi.org/10.3390/nano13091578.
25. Sharma, Priyanka R., et al. "Chapter 5 - Nanocellulose in Membrane Technology for Water Purification." Separation Science and Technology, edited by Satinder Ahuja, vol. 15, Academic Press, 2022, pp. 69–85. https://doi.org/10.1016/B978-0-323-90763-7.00011-1.
26. Gopal, Renuga, et al. "Electrospun Nanofibrous Filtration Membrane." Journal of Membrane Science, vol. 281, no. 1, Sept. 2006, pp. 581–86. https://doi.org/10.1016/j.memsci.2006.04.026.
27. Guo, Xiaoyan, et al. "Engineering Polydopamine-Glued Sandwich-like Nanocomposites with Antifouling and Antibacterial Properties for the Development of Advanced Mixed Matrix Membranes." Separation and Purification Technology, vol. 237, 2020. https://doi.org/10.1016/j.seppur.2019.116326.
28. Gopakumar, Deepu, et al. Nanocellulose-Based Membranes for Water Purification. 2019, pp. 59–85. https://doi.org/10.1016/B978-0-12-813926-4.00004-5.
29. Naseer, Ayesha. "Role of Nanocomposites and Nano Adsorbents for Heavy Metals Removal and Dyes. An Overview." Desalination and Water Treatment, vol. 320, Oct. 2024, p. 100662. https://doi.org/10.1016/j.dwt.2024.100662.
30. Morsi, Rania E., et al. "Influence of the Fabrication Conditions on the Physical Properties and Water Treatment Efficiency of Cellulose Acetate Porous Membranes." Water, vol. 15, no. 6, Jan. 2023, p. 1061. https://doi.org/10.3390/w15061061.
31. Liu, Dongyan, et al. "5 - Electrospun Polymeric Composite Nanofibers with Cellulose Nanocrystals and Their Applications." Electrospun Polymers and Composites, edited by Yu Dong et al., Woodhead Publishing, 2021, pp. 147–78. https://doi.org/10.1016/B978-0-12-819611-3.00005-4.
32. Li, Han, et al. "Cellulose Nanofiber-Assisted Dispersion of Halloysite Nanotubes via Silane Coupling Agent-Reinforced Starch–PVA Biodegradable Composite Membrane." Membranes, vol. 12, no. 2, Feb. 2022, p. 169. https://doi.org/10.3390/membranes12020169.
33. Mu, Keguang, et al. "Enhanced Permeability and Antifouling Performance of Cellulose Acetate Ultrafiltration Membrane Assisted by L-DOPA Functionalized Halloysite Nanotubes." Carbohydrate Polymers, vol. 174, Oct. 2017, pp. 688–96. https://doi.org/10.1016/j.carbpol.2017.06.089.
34. Güneş-Durak, Sevgi, et al. "Mechanical Enhancement and Water Treatment Efficiency of Nanocomposite PES Membranes: A Study on Akçay Dam Water Filtration Application." ACS Omega, vol. 9, no. 29, July 2024, pp. 31556–68, https://doi.org/10.1021/ACSOMEGA.4C01410.
35. Rahbari-Sisakht, Masoud, et al. "Thin-Film Nanocomposite Membranes for Water Treatment: Evolution, Applications, Challenges, and Advancement Strategies." Journal of Environmental Chemical Engineering, vol. 13, no. 3, June 2025, p. 116392. https://doi.org/10.1016/j.jece.2025.116392.
36. Sadare, Olawumi O., et al. "Lignocellulosic Biomass-Derived Nanocellulose Crystals as Fillers in Membranes for Water and Wastewater Treatment: A Review." Membranes, vol. 12, no. 3, Mar. 2022, p. 320. https://doi.org/10.3390/membranes12030320.
37. Acarer Arat, Seren, et al. "Effect of Promising Sustainable Nano-Reinforcements on Polysulfone/Polyvinylpyrrolidone-Based Membranes: Enhancing Mechanical Properties and Water Filtration Performance." Polymers, vol. 16, no. 24, Jan. 2024, p. 3531. https://doi.org/10.3390/polym16243531.
38. Carpenter, Alexis Wells, et al. "Cellulose Nanomaterials in Water Treatment Technologies." Environmental Science & Technology, vol. 49, no. 9, May 2015, pp. 5277–87. https://doi.org/10.1021/es506351r.
39. Raji, Zarifeh, et al. "Adsorption of Heavy Metals: Mechanisms, Kinetics, and Applications of Various Adsorbents in Wastewater Remediation—A Review." Waste, vol. 1, no. 3, Sept. 2023, pp. 775–805. https://doi.org/10.3390/waste1030046.
40. Chen, Hsin-Chen, et al. "Effects of Nanocellulose Formulation on Physicomechanical Properties of Aquazol–Nanocellulose Composites." Cellulose, vol. 27, no. 10, July 2020, pp. 5757–69. https://doi.org/10.1007/s10570-020-03190-x.
41. Saljoughi, Ehsan, et al. "Cellulose Acetate (CA)/Polyvinylpyrrolidone (PVP) Blend Asymmetric Membranes: Preparation, Morphology and Performance." Desalination, vol. 249, no. 2, Dec. 2009, pp. 850–54. https://doi.org/10.1016/j.desal.2008.12.066.
42. Tao, Mi-mi, et al. "Effect of Solvent Power on PVDF Membrane Polymorphism during Phase Inversion." Desalination, vol. 316, May 2013, pp. 137–45. https://doi.

org/10.1016/j.desal.2013.02.005.
43. Bai, Langming, et al. "Surface Coating of UF Membranes to Improve Antifouling Properties: A Comparison Study between Cellulose Nanocrystals (CNCs) and Cellulose Nanofibrils (CNFs)." Chemosphere, vol. 217, Feb. 2019, pp. 76–84. https://doi.org/10.1016/j.chemosphere.2018.10.219.
44. Zhou, Zongyao, et al. "Carbon Nanotube-Supported Polyamide Membrane with Minimized Internal Concentration Polarization for Both Aqueous and Organic Solvent Forward Osmosis Process." Journal of Membrane Science, vol. 611, Oct. 2020, p. 118273. https://doi.org/10.1016/j.memsci.2020.118273.
45. Dharini, V., et al. "PVA/Essential Oil-Based Active Food Packaging Films Functionalised with Halloysite Nanotubes and Cellulose Nanocrystals as Filler Materials for the Shelf-Life Extension of Papaya Fruits." International Journal of Food Science & Technology, vol. 59, no. 1, 2024, pp. 318–32. https://doi.org/10.1111/ijfs.16811.
46. Gao, Haiping, et al. "Hybrid Dimensional MXene/CNC Framework-Regulated Nanofiltration Membrane with High Separation Performance." ACS ES&T Water, vol. 3, no. 7, July 2023, pp. 1767–77. https://doi.org/10.1021/acsestwater.2c00231.
47. Amjadi, Mohammad, et al. "A Composite Prepared from Halloysite Nanotubes and Magnetite (Fe3O4) as a New Magnetic Sorbent for the Preconcentration of Cadmium(II) Prior to Its Determination by Flame Atomic Absorption Spectrometry." Microchimica Acta, vol. 182, no. 9, July 2015, pp. 1627–33. https://doi.org/10.1007/s00604-015-1491-y.
48. Silva, Philipe Augusto Pocidonio, et al. Bio-Sorbent from Castor Oil Polyurethane Foam Containing Cellulose-Halloysite Nanocomposite for Removal of Manganese, Nickel and Cobalt Ions from Water. 4363347, Social Science Research Network, 18 Feb. 2023. https://doi.org/10.2139/ssrn.4363347.
49. Choi, Hyeong Yeol, et al. "Thiol-Functionalized Cellulose Nanofiber Membranes for the Effective Adsorption of Heavy Metal Ions in Water." Carbohydrate Polymers, vol. 234, Apr. 2020, p. 115881. https://doi.org/10.1016/j.carbpol.2020.115881.
50. Yong, Wai Fen, et al. "New Polyethersulfone (PESU) Hollow Fiber Membranes for CO2 Capture." Journal of Membrane Science, vol. 552, Apr. 2018, pp. 305–14. https://doi.org/10.1016/j.memsci.2018.02.008.
51. Chang, Hailin, et al. "Effects of Organics Concentration on the Gravity-Driven Membrane (GDM) Filtration in Treating Iron- and Manganese-Containing Surface Water." Water Research, vol. 226, Nov. 2022, p. 119223. https://doi.org/10.1016/j.watres.2022.119223.
52. Tang, Xiaobin, et al. "Gravity-Driven Membrane Filtration Treating Manganese-Contaminated Surface Water: Flux Stabilization and Removal Performance." Chemical Engineering Journal, vol. 397, Oct. 2020, p. 125248. https://doi.org/10.1016/j.cej.2020.125248.
53. Buamah, R. Adsorptive Removal of Manganese, Arsenic and Iron from Groundwater. Doctor of Philosophy, Wageningen University, [S.l.], Oct. 2009. https://doi.org/10.18174/340409.
54. Pascu, Daniela-Elena, et al. "Iron and Manganese Removal from Drinking Water." Journal of Electrochemical Science and Engineering, vol. 6, no. 1, Apr. 2016, pp. 47–55. https://doi.org/10.5599/jese.244.